

Small-Scale Cosmic Microwave Background Polarization from Reionization

Daniel Baumann^{1,2}, Asantha Cooray¹, and Marc Kamionkowski¹

¹*California Institute of Technology, Mail Code 130-33, Pasadena, CA 91125*

²*University of Cambridge, Cambridge, CB3 0HE*

E-mail: (db275,asante,kamion)@tapir.caltech.edu

We discuss fluctuations in the cosmic microwave background (CMB) polarization due to scattering from reionized gas at low redshifts. Polarization is produced by re-scattering of the primordial temperature anisotropy quadrupole and of the kinematic quadrupole that arises from gas motion transverse to the line of sight. We show that both effects produce equal E- and B-parity polarization, and are, in general, several orders of magnitude below the dominant polarization contributions at the last scattering surface to E-modes or the gravitational-lensing contribution to B-modes at intermediate redshifts. These effects are also several orders of magnitude below the B polarization due to lensing even after subtraction with higher-order correlations, and are thus too small to constitute a background for searches for the polarization signature of inflationary gravitational waves.

I. INTRODUCTION

The angular power spectrum of cosmic microwave background (CMB) temperature fluctuations is now becoming a powerful cosmological probe [1], both due to our detailed understanding of physics during the recombination era [2] and progress on the experimental front [3]. In addition to the primary anisotropies generated at the last-scattering surface, CMB photons are also affected by large-scale structure at low redshifts. These latter contributions result from scattering off free electrons in clusters or the reionized IGM and from modifications due the evolving gravitational field associated with the formation of structures [4].

The existence of such secondary signals has now become evident with the recent detection of small-scale power in excess of that from primary fluctuations [5]. The simplest and most plausible explanation for this small-scale power is the Sunyaev-Zel'dovich (SZ; [6]), re-scattering of CMB photons from hot electrons in unresolved galaxy clusters. Although the power observed is considerably larger than theoretical expectations, the excess can be accommodated with a relatively small increase in the power-spectrum amplitude [7–10].

In addition to small-scale anisotropies in the temperature, increasing attention is now being devoted to detection of the CMB polarization. Besides resolving cosmological parameter degeneracies [1], the polarization will allow several unique cosmological and astrophysical studies to be carried out. These include a reionization signal [11], probes of gravitational lensing [12], and a signature of inflationary gravitational waves (IGW) through its contribution to the B, or curl, modes of the polarization [13].

Given the rapid pace of experimental progress and the rule of thumb that the polarization is typically 10% of the temperature anisotropy, it is appropriate to investigate the polarization produced by the secondary effects that have produced the recently detected small-scale power. This polarization is produced by Thomson scattering of

the quadrupole moment of the radiation incident on the scatterer. The quadrupole moment can be either the primordial quadrupole that the scatterer sees [14] or the kinematic quadrupole that arises from quadratic terms in the Doppler shift when the gas moves transverse to the line of sight [6]. Small-scale angular fluctuations in this polarization are produced by variations in the optical depth as a function of position across the sky.

Since the secondary polarization signals can affect cosmological studies involving the primordial polarization, and, by themselves, may provide important information on astrophysics at late times, it is important that we both quantify and understand the extent to which large-scale structure can be a potential source of CMB polarization. Here, we discuss the angular power spectra for scattering from reionized electrons and study how these may affect potentially interesting studies with CMB polarization.

Our calculation parallels that of Ref. [15], although differs in that we present a simplified derivation of the results based on a flat-sky approximation and use a halo-clustering approach [16] to describe fluctuations in the electron density, in analogy to similar recent calculations of small-scale temperature fluctuations from unresolved clusters [8,17,18]. We also include for the first time the frequency dependence in the small-scale polarization using results for the polarization from individual clusters [19,20].

The paper is organized as follows. In § II, we introduce polarization signals associated with the scattering of the primordial CMB temperature quadrupole and with the kinematic quadrupole generated by transverse motions. We then display and discuss our results in § III. Though we present a general discussion of the polarization, when illustrating results, we will use the currently favored Λ CDM cosmology with matter density (in units of the critical density) $\Omega_m = 0.35$, baryon density $\Omega_b = 0.05$, vacuum-energy density $\Omega_\Lambda = 0.65$, Hubble constant (in units of $100 \text{ km sec}^{-1} \text{ Mpc}^{-1}$) $h = 0.65$, and spectral $n = 1$ for primordial density perturbations. We employ natural units with the speed of light $c = 1$ throughout.

II. POLARIZATION POWER SPECTRA

If the radiation incident on a reionized electron has a nonzero quadrupole moment, then the scattered radiation will be linearly polarized. The two dominant origins for this quadrupole moment are: (a) A quadrupole from primordial CMB fluctuations, and (b) a quadrupole from the quadratic term in the Doppler shift if the scattering gas has a transverse velocity.

The statistics of the polarization produced in this way is inherently non-Gaussian: Although the amplitude of the polarization in a given direction is determined by the optical depth to Thomson scattering, the orientation is determined by the radiation quadrupole incident on the scattering gas. The power spectrum is thus in principle determined by a convolution of the optical-depth field with the quadrupole field.

In practice, however, we simplify by assuming that the quadrupole moment is smooth over large distances, and that there are small-scale variations only in the free-electron density. We can then proceed to calculate the polarization fluctuations that are linear in the electron-density fluctuations. The correlation length of the CMB quadrupole is comparable to the horizon, and so our assumptions are fully justified for this case, as long as we restrict our attention to multipole moments $l \gtrsim 10$. On the other hand, the peculiar velocity is correlated only on much smaller scale, ~ 60 Mpc in our fiducial Λ CDM cosmology. Our calculations of the polarization power spectrum for the kinematic quadrupole will thus be reliable only for scales smaller than this, or multipole moments $l \gtrsim 100$.

We first discuss the power spectra. A polarization map will consist of a measurement of the Stokes parameters $Q(\hat{\mathbf{n}})$ and $U(\hat{\mathbf{n}})$ as functions of position $\hat{\mathbf{n}}$ on some patch of the sky. We can construct Fourier components $Q(\mathbf{l})$ and $U(\mathbf{l})$ by

$$X(\mathbf{l}) = \int d^2\hat{\mathbf{n}} e^{i\mathbf{l}\cdot\hat{\mathbf{n}}} X(\hat{\mathbf{n}}), \quad (1)$$

where $X \equiv Q, U$, and \mathbf{l} is a vector in the plane of a region of the sky sufficiently small to be considered flat. Since the Stokes parameters Q and U depend on the choice of axes, we consider the rotationally invariant combinations,

$$\begin{aligned} E(\mathbf{l}) &= \cos(2\phi_1)Q(\mathbf{l}) + \sin(2\phi_1)U(\mathbf{l}) \\ B(\mathbf{l}) &= \cos(2\phi_1)U(\mathbf{l}) - \sin(2\phi_1)Q(\mathbf{l}), \end{aligned} \quad (2)$$

where ϕ_1 is the angle between \mathbf{l} and the chosen x-axis in the plane of the sky. We define the angular power spectra C_l^{EE} and C_l^{BB} from

$$\langle Y(\mathbf{l})Y(\mathbf{l}') \rangle = (2\pi)^2 \delta_D(\mathbf{l} + \mathbf{l}') C_l^{YY}, \quad (3)$$

where $Y \equiv E, B$, and the angle brackets denote an average over all realizations of the density field.

As discussed above, we suppose that the radiation quadrupole moment is smooth over the region of sky we are considering. If so, then

$$\begin{aligned} \langle E(\mathbf{l})E(\mathbf{l}') \rangle &= \langle B(\mathbf{l})B(\mathbf{l}') \rangle \\ &= \frac{1}{2} (\langle Q(\mathbf{l})Q(\mathbf{l}') \rangle + \langle U(\mathbf{l})U(\mathbf{l}') \rangle), \end{aligned} \quad (4)$$

while

$$\langle E(\mathbf{l})B(\mathbf{l}') \rangle = \frac{1}{2} (\langle Q(\mathbf{l})U(\mathbf{l}') \rangle - \langle Q(\mathbf{l}')U(\mathbf{l}) \rangle) = 0, \quad (5)$$

where the latter equality is consistent with parity conservation. These results can be derived by noting that if the quadrupole moment is constant, then the orientation of the polarization is constant. If so, we may choose our axes on the sky so that $U = 0$. Then, $E(\mathbf{l}) \propto \sin(2\phi_1)$, and $B(\mathbf{l}) \propto \cos(2\phi_1)$, but when averaged over the orientation angle ϕ_1 , we recover Eq. (4).

We now proceed to calculate the power spectra induced by reionization. The polarization in direction $\hat{\mathbf{n}}$ due to scattering from free electrons is an integral along the line of sight [21],

$$Q(\hat{\mathbf{n}}) - iU(\hat{\mathbf{n}}) = \sqrt{\frac{3}{40\pi}} \int dr \frac{d\tau(r\hat{\mathbf{n}}, r)}{dr} a_{22}(r), \quad (6)$$

where r is the comoving distance, $(d\tau/dr)(r\hat{\mathbf{n}}, r) = \sigma_T n_e(r\hat{\mathbf{n}}, r) a(r)$, $a(r)$ is the scale factor at a comoving distance r , $n_e(r\hat{\mathbf{n}}, r)$ is the free-electron density at direction $\hat{\mathbf{n}}$ at distance r , and σ_T is the Thomson cross section.

In Eq. (6), $a_{22}(r)$ is the radiation quadrupole moment at distance r . More precisely, $a_{22}(r)$ is the coefficient of the spherical harmonic $Y_{22}(\theta, \phi)$ in a spherical-harmonic expansion of the radiation intensity in a coordinate system in which the line of sight is the $\hat{\mathbf{z}}$ direction. Note that we take $a_{22}(r)$ to be a function of distance only, and not direction, consistent with our assumption that the quadrupole is coherent over a large patch of the sky. Since we use Limber's approximation below, in which angular correlations are induced only by spatial separations at the same distance, the variation of $a_{22}(r)$ with distance can be included consistently.

With the polarization written as a projection, Eq. (6), along the line of sight, the angular power spectrum follows in the flat-sky limit from Limber's equation [22],

$$\begin{aligned} C_l^{EE} &= C_l^{BB} \\ &= \frac{3}{80\pi} \int_0^{z_{\text{rei}}} dz \frac{d^2V}{d\Omega dz} |a_{22}(z)|^2 P_{\tau\tau}^{(t)} \left(\frac{l}{d_A}, z \right), \end{aligned} \quad (7)$$

where $P_{\tau\tau}^{(t)}$ is the power spectrum of $d\tau/dr$, proportional to the power spectrum of the electron density n_e , and the integral is taken up to the redshift z_{rei} of reionization using the comoving differential volume given by $d^2V/d\Omega dz$.

We now assume that the free-electron density is distributed like the mass in the Universe and model the mass

distribution following the halo approach to large-scale structure [16]. We thus decompose the power spectrum into two parts, one that describes contributions from single halos (1-halo term) and a part that accounts for correlations between halos (2-halo term) [8,17,18,23]:

$$P_{\tau\tau}^{(t)} = P_{\tau\tau}^{1h} + P_{\tau\tau}^{2h}, \quad (8)$$

where

$$\begin{aligned} P_{\tau\tau}^{1h}(k, z) &= \int dM \frac{dn(M, z)}{dM} |\tau_l(M, z)|^2, \\ P_{\tau\tau}^{2h}(k, z) &= P^{\text{lin}}(k, z) \\ &\times \left[\int dM \frac{dn(M, z)}{dM} b(M, z) \tau_l(M, z) \right]^2. \end{aligned} \quad (9)$$

Here, $(dn/dM)(M, z)$ is the mass function of halos [24] and $b(M, z) = 1 + \frac{\nu^2(M, z) - 1}{\delta_c}$ is the halo bias [25] with $\nu(M, z) = \delta_c / \sigma(M, z)$ the peak-height threshold with rms fluctuation within a top-hat filter at the virial radius corresponding to mass M given by $\sigma(M, z)$ and threshold overdensity of spherical collapse given by δ_c . Useful fitting functions for these quantities are tabulated in Ref. [26].

We define the projected scattering optical depth as $\tau(\theta) = \sigma_T \int n_e(y, \theta) dy$ where y is the line-of-sight distance along each halo at angular distance θ from the cluster center. The two-dimensional Fourier transform of $\tau(\theta)$ is,

$$\tau_l = 2\pi \int_0^{\theta_{\text{vir}}} \theta d\theta \tau(\theta) J_0(l\theta), \quad (10)$$

where θ_{vir} corresponds to the virial radius of the halo. For simplicity, we model the electron distribution within each halo using a β -profile and normalize it such that the gas mass fraction of each halo produces the global baryon fraction [17]. Finally, $P^{\text{lin}}(k)$ is the power spectrum of the linear density field. We use the formulae of Ref. [27] to describe the transfer function and normalize the power spectrum to match $\sigma_8 = 0.9$ consistent with COBE fluctuations at large scales [28]. We comment below on the σ_8 dependence of our results.

A. Primordial Quadrupole

The primordial quadrupole will have a coherence length comparable to the horizon. We thus expect that the amplitude of the polarization power spectrum measured on a $\mathcal{O}(10^\circ)$ patch of sky may differ by order unity from that on a different $\mathcal{O}(10^\circ)$ patch of sky (and likewise that our calculation should break down for $l \lesssim 10$). However, when averaged over the entire sky, the amplitude of the power spectrum should be given by replacing the quantity $|a_{22}(z)|^2$ in Eq. (7) by its expectation value, $C_2^{\Theta\Theta}(z)$, the variance of the temperature

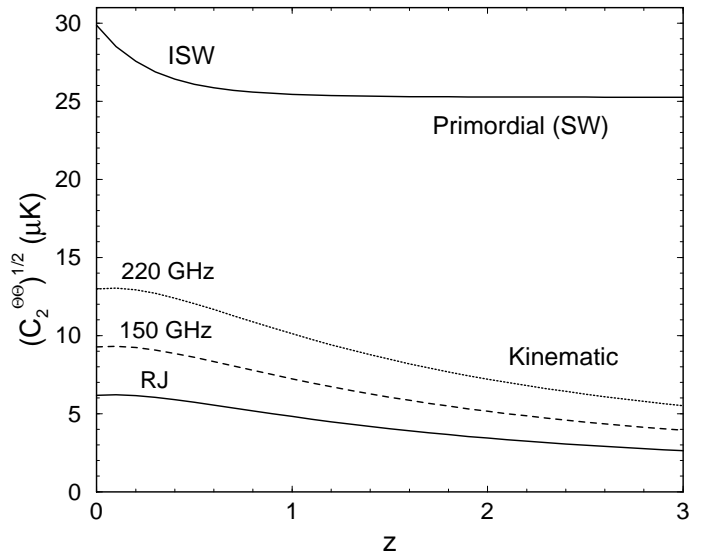


FIG. 1. The temperature quadrupole, $C_2^{\Theta\Theta}$, as a function of redshift. We show both the primordial and the kinematic quadrupole. The bottom kinematic-quadrupole curve is for $g(x) = 1$, as appropriate for the Rayleigh-Jeans (RJ) part of the frequency spectrum, and the dashed and dotted curves are, respectively, for frequencies 150 and 220 GHz.

quadrupole at redshift z . At redshift $z = 0$, with the power-spectrum tilt fixed at unity, COBE finds $C_2^{\Theta\Theta}(z = 0) = (27.5 \pm 2.4 \mu\text{K})^2$ [29]. At higher redshifts, the mean quadrupole moment evolves due to the integrated Sachs-Wolfe effect and possibly, if the power spectrum is not flat, due to any scale dependence since the quadrupole probes smaller distances at earlier times. We calculate $C_2^{\Theta\Theta}(z)$ following Ref. [15] for our fiducial Λ CDM cosmology and show the result in Fig. 1.

Finally, note that Thomson scattering from cold electrons will not change the photon frequency. Thus, there will be no frequency dependence of the primordial quadrupole if we use Stokes parameters in temperature units—rather than the intensity units used by Ref. [19]—as we do throughout this paper.

B. Kinematic Quadrupole

As discussed in Ref. [6], an electron gas moving with a transverse velocity v_t relative to the CMB rest frame sees an a_{22} quadrupole moment (in a coordinate system in which z is along the line of sight),

$$a_{22} = g(x) \sqrt{\frac{4\pi}{30}} v_t^2 e^{2i\phi_v}, \quad (11)$$

where ϕ_v is the orientation angle for v_t on the plane of the sky. To obtain this result, note that in a coordinate system in which the \hat{z} axis is aligned with the cluster's motion, the quadrupole dependence of the radiation temperature is $g(x)v_t^2(\mu^2 - 1/3) = g(x)v_t^2(2/3)\sqrt{4\pi/5}Y_{2,0}$,

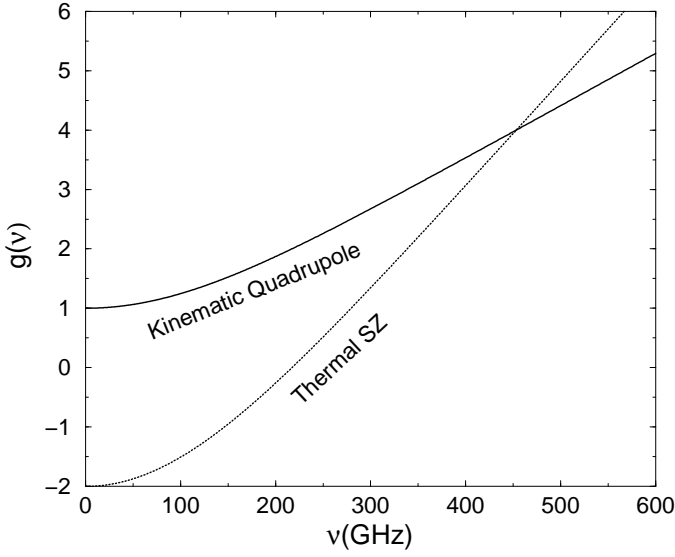


FIG. 2. The solid curve shows the frequency spectrum of the kinematic temperature (rather than intensity) quadrupole. For reference, we also show the spectral dependence of the SZ thermal effect with the dotted curve.

where μ is the cosine of the angle between the radiation direction and the $\hat{\mathbf{z}}$ direction. However, in a coordinate system in which the $\hat{\mathbf{z}}$ axis is taken to be along the line of sight, $(\mu^2 - 1/3) = -(1/3)\sqrt{4\pi/5}Y_{2,0} + \sqrt{2\pi/15}(Y_{2,2} + Y_{2,-2})$. Thus, the coefficient of $Y_{2,2}$, the component of the quadrupole moment that gives rise to polarization in our direction, is only a fraction $\sqrt{3/8}$ of the total quadrupole moment.

Unlike the primordial quadrupole, the kinematic quadrupole has a frequency dependence which we denote by $g(x)$, where $x = h\nu/kT_{\text{CMB}}$. Following Refs. [19,20], this frequency dependence can be calculated by expanding the spectral intensity distribution of the CMB in the rest frame of electrons, $I_\nu \propto x^3/(e^{x\gamma(1+v\mu)} - 1)$, in terms of velocity v , with $\gamma = (1-v^2)^{-1/2}$ and μ the cosine of the angle between velocity and incident photon direction. We then obtain the frequency dependence of the quadrupole term, in temperature units instead of intensity units, to be $g(x) = (x/2) \coth(x/2)$. In Fig. 2, we show the frequency dependence of the kinematic quadrupole, which was neglected in Ref. [15] *. For reference, we also plot the frequency dependence of the thermal Sunyaev-Zel'dovich effect,

The bulk flows associated with large-scale structure have coherence scales of order ~ 60 Mpc. At first, we might be tempted to think that if we were to survey some region of sky small compared with the coherence length $\sim 1^\circ$ for the peculiar velocity when projected at a

typical redshift of order unity, then the power-spectrum amplitude might generally differ by order unity from the power-spectrum amplitude on some other similarly sized patch of sky. This would be true if all the fluctuations were produced at one distance. However, since there will be $\mathcal{O}(100)$ 60-Mpc coherence patches along the line of sight, these will tend to average out, and the polarization power-spectrum amplitude should be roughly the same from one 1° degree patch to another. It is thus appropriate to replace $|a_{22}(z)|^2$ in Eq. (7) by its expectation value,

$$\langle |a_{22}|^2 \rangle = \frac{4\pi}{30} g^2(x) \langle v_t^4 \rangle = \frac{16\pi}{135} g^2(x) v_{\text{rms}}^4, \quad (12)$$

where we have used $\langle v_t^4 \rangle = \langle (v_x^2 + v_y^2)^2 \rangle = (8/9)v_{\text{rms}}^4$, since $\langle v_x^2 \rangle = \langle v_y^2 \rangle = v_{\text{rms}}^2/3$, $\langle v_x^4 \rangle = \langle v_y^4 \rangle = 3\langle v_x^2 \rangle^2 = v_{\text{rms}}^2/3$, and $\langle v_x^2 v_y^2 \rangle = \langle v_x^2 \rangle \langle v_y^2 \rangle = v_{\text{rms}}^4/9$. We calculate the linear-theory rms peculiar velocity from

$$v_{\text{rms}}^2(r) = \int \frac{k^2 dk}{2\pi^2} \left(\frac{\dot{G}}{k} \right)^2 P^{\text{lin}}(k, 0), \quad (13)$$

where G is the linear-theory density-perturbation growth factor, and the overdot represents a derivative with respect to radial distance. According the halo-clustering model [16], peculiar-velocity fields are correlated over large distances and the nonlinear corrections to v_{rms}^2 are small. The resulting linear-theory rms kinematic quadrupole is also shown in Fig. 1 assuming $g(x) = 1$ as relevant for Rayleigh-Jeans (RJ) part of the frequency spectrum when $x \rightarrow 0$, and for $\nu = 150$ GHz and $\nu = 220$ GHz.

Before moving on to discuss our results, a few words on how our derivations compare with those of Hu [15] are necessary. Note that our Eq. (7) agrees with Eq. (63) of Ref. [15] after converting to the logarithmic power spectrum, $\Delta^2(k) = k^3 P(k)/2\pi^2$, using Limber's approximation with $k = l/d_A$, and substituting $|a_{22}(z)|^2 = (4\pi/5)Q_{\text{rms}}^2$ for the temperature quadrupole. Similarly, our derivation for the polarization power spectrum due to the kinematic quadrupole agrees with that of Ref. [15], though this comparison requires an additional step. The kinematic quadrupole which replaces Q_{rms}^2 in Eq. (63) of Ref. [15] is given in Eq. (58) as $(8/45)(1 - f_{\text{kin}})v_{\text{rms}}^4$. The factor f_{kin} accounts for mode coupling associated with the velocity field and is given by the mode-coupling integral in the second line of Eq. (58) of Ref. [15]. If we take the limiting case of f_{kin} with $y_1 \ll 1$ and $y_2 \rightarrow 1$, such that the two velocity power spectra decouple from each other, then $f_{\text{kin}} = 1/6$ exactly and the relevant kinematic quadrupole becomes $(8/54)v_{\text{rms}}^4$. This is consistent with Eq. (12) of this paper. This can be verified by substituting our Eq. (12) into our Eq. (7), which recovers Eq. (64) of Ref. [15]. The fact that Hu finds numerically that $f_{\text{kin}} = 1/6$ to a very good approximation justifies our assumption that the velocity and density fields are effectively decoupled.

*Note that our Figure for the frequency dependence differs from Fig. 4 of Ref. [19] due to our use of temperature units and their use of intensity units.

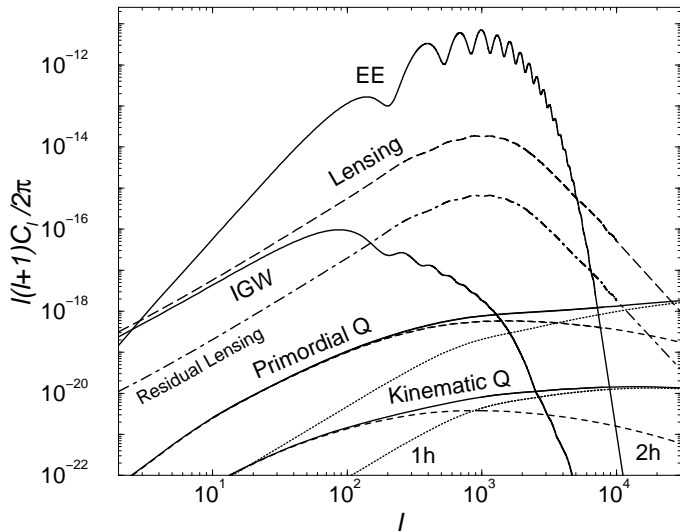


FIG. 3. Polarization power spectra due to the rescattering of the primordial and kinematic quadrupoles. We break total power in each of these cases into the 1- (1h; dotted lines) and 2-halo (2h; dashed lines) terms under the halo-based approach used here. While at large angular scales correlations between halos dominate, at small angular scales of order few arcminutes and below, contributions are dominated by the 1-halo term. For comparison, we also show primordial polarization power spectra for E and B-modes involving dominant scalar (E-mode) and tensor (B-mode) contributions respectively. The tensor contribution to B-modes due to inflationary gravitational waves (IGW) assumes an energy scale for inflation of 10^{16} GeV. The long-dashed curve is the contribution to B-modes of polarization resulting from the cosmic shear conversion of power in E-modes, while the dot-dashed line labeled “Residual Lensing” represents the noise contribution after optimally subtracting the lensing contribution using higher order statistics (see text for details).

III. RESULTS AND DISCUSSION

We summarize our results on the polarization power spectra in Fig. 3. Note that the secondary polarization discussed here contributes equally to E- and B-modes. While the 1-halo term dominates at arcminute angular scales and below, correlations between halos are important and determine the total effect due to secondary polarization at angular scales corresponding to a few degrees. The dependence of our results on the inclusion of the 2-halo term is consistent with the result obtained for the temperature power spectra from the kinetic SZ effect [30], while it is inconsistent with the thermal SZ effect, where contributions are dominated by the 1-halo term over the whole range of angular scales. The latter behavior is explained by the fact that the thermal-SZ effect is highly dependent on the most massive halos, while the kinetic SZ effect, and the secondary polarization signals calculated here, are *independent* of the gas temperature and thus can depend on halos with a wider mass range.

As shown in Fig. 3, the secondary E-mode polarization

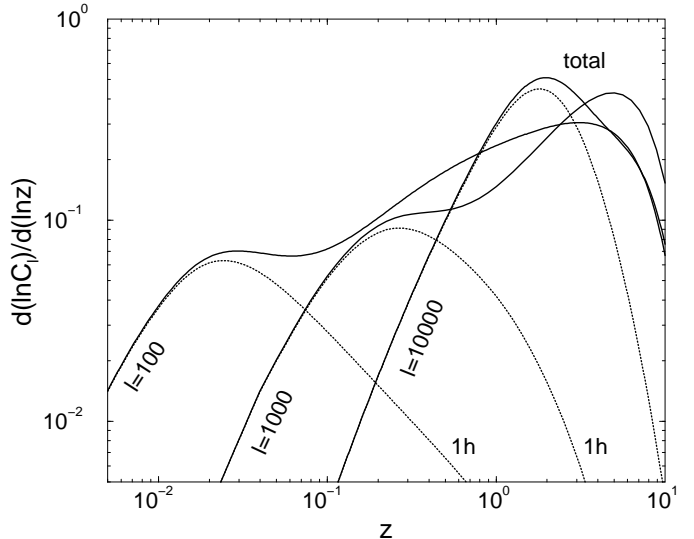


FIG. 4. The fractional contribution to polarization power spectra due to scattering of the primary anisotropy temperature quadrupole as a function of redshift. Here, we plot $d \ln C_l / d \ln z$, for three specific values of l (10^2 , 10^3 , and 10^4). We show the total (solid curves) as well as the 1-halo term (dotted curves). Note that contributions come from a broad range in redshift, while, with increasing l , or decreasing angular scale, fractional contributions in the 1-halo term increase to higher redshifts.

is several orders of magnitude below the E polarization from the surface of last scattering. The secondary polarization is therefore unlikely to be a source of confusion when interpreting polarization contributions to E modes. The amplitude of the primary effect in B modes, due to gravitational waves, is highly uncertain and depends on the energy scale of inflation [31]. For illustration, we show in Fig. 3 the inflationary gravitational wave (IGW) signal assuming an energy scale for inflation of $E_{\text{infl}} = 10^{16}$ GeV; the amplitude of the power spectrum scales as E_{infl}^4 . At large angular scales the secondary polarization is several orders of magnitude below the peak of this hypothetical IGW polarization signal. If the energy scale of inflation is lowered considerably, say to $E_{\text{infl}} \lesssim 10^{15}$ GeV, then we might guess that the secondary polarization could ultimately constitute a background.

As also shown in Fig. 3, however, there is a contribution to the B-mode power spectrum that arises from conversion of the primary E modes to B modes by gravitational lensing [12], and this is considerably larger than the secondary polarization. Moreover, we also show (the dot-dash curve) the contribution to the irreducible B-mode power spectrum that remains even after the lensing has been optimally subtracted with higher-order correlations [32–35]. This residual lensing power spectrum is considerably larger than the polarization from reionization. If the power spectrum is measured at a frequency $\nu \simeq 220$ GHz, then the polarization power spectrum from the kinematic effect will be boosted by a factor ~ 5 from

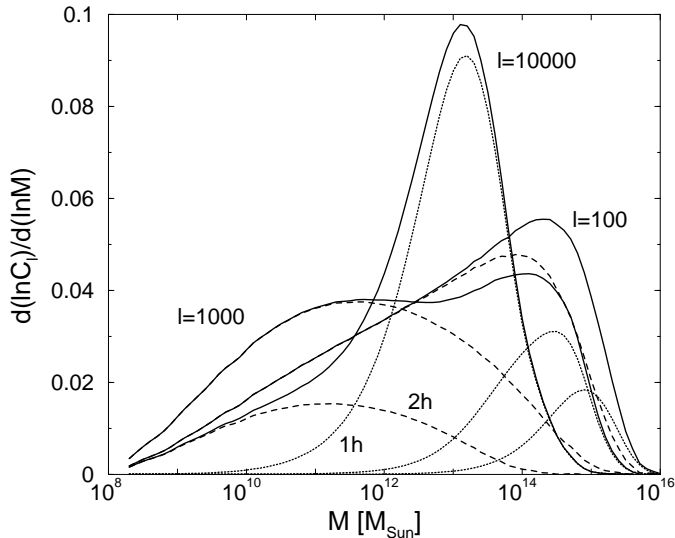


FIG. 5. The fractional contribution to polarization power spectra due to scattering of the primary anisotropy temperature quadrupole as a function of cluster mass (in terms of solar mass). Here, we plot $d \ln C_l / d \ln M$, for three specific values of l (10^2 , 10^3 , and 10^4). We show the total (solid line), the 1-halo term (dotted), and the 2-halo term (dashed).

the $g(x) = 1$ power spectrum shown in Fig. 3. Moreover, if $\sigma_8 = 1$ (rather than the value $\sigma_8 = 0.9$ assumed in Fig. 3), then both the secondary power spectra will be increased for the same reasons that the temperature power spectra increase by a factor ~ 3 .[†] Even with the possible frequency and σ_8 boosts, the secondary effects we consider here will be unlikely to be a factor for either gravitational-lensing or gravitational-wave studies with B modes.

In Fig. 4, we show the fractional contributions to polarization power spectra associated with the scattering of the temperature quadrupole as a function of redshift. We show the total and the 1-halo term for three specific values of l corresponding to degree scales to arcminute angular scales. Though not shown here, we find consistent behavior for the polarization power spectrum generated by the scattering of the kinematic quadrupole. As shown, contributions come over a broad range in redshift out to the assumed reionization redshift of 10 with a decrease at highest redshifts due to the decreasing abundance of massive halos at higher redshifts. At arcminute scales with $l \sim 10^4$, the signal arises from halos at $z > 1$. A comparison of this behavior to Fig. 1 reveals that at redshifts greater than 1, the primary temperature quadrupole at the cluster positions results from a projection of the SW

effect only. Thus, at small angular scales, scattering contributions come only from the quadrupole associated with the SW effect and not the total that includes the ISW effect as well.

In Fig. 5, we show the mass dependence of the secondary polarization signal, again using the scattering of the temperature quadrupole for illustration purposes. We show the total, the 1-halo, and the 2-halo term at three different values of l . While the 1-halo term is dominated by halos at the high-mass end of the mass function, the 2-halo term arises from a wide range in halo mass. At tens of arcminute scales equal contributions come from halo masses in the range of 10^{10} to $10^{14} M_\odot$. This is consistent with the equivalent result for the kinetic SZ effect where a wide range of masses contribute.

Note that in addition to the auto-correlation of polarization, one expects secondary temperature fluctuations due to galaxy clusters to be correlated with that of the secondary polarization involving the E-mode. The temperature-polarization cross-correlation with the B-modes is expected to be zero based on parity considerations. We considered all combinations between secondary polarization and temperature anisotropies involving thermal and kinetic SZ effects and found them to be zero based on simple geometric arguments.

While our simple flat-sky derivation of the secondary polarization anisotropy from reionization agrees with the all-sky approach of Ref. [15], our calculational method complements the one used there. We use the halo model to describe the non-linear power spectrum of electrons while in Ref. [15], electrons of the intergalactic medium were assumed to trace the dark-matter-density field. Our numerical results agree well with those of Ref. [15], particularly at large angular scales where they should both converge to the same linear-theory calculation. Here we have neglected to consider the expected smoothing of the electron density on small scales from reheating of the IGM gas. However, as Ref. [15] shows, these effects are easily included and reduce the power spectrum substantially only on angular scales $l \gtrsim 10^4$ smaller than those we have considered here.

While our halo-based approach is likely to be affected by uncertainties related to the mass function or the distribution of electrons within halos, we expect our calculations to accurately reflect the polarization anisotropy power at small angular scales. In the case of the kinematic quadrupole, it is likely that we have overestimated the power at scales of a few degrees or more due to our assumption that the velocity field is coherent at such angular scales. We expect this assumption to only affect the 2-halo term of correlations and to result in an overestimate of C_l when l is less than ~ 1000 .

[†]However, the boost in the polarization power spectra will be smaller due to the fact that much of the polarization is induced by electrons in smaller halos, rather than the massive clusters that induce the temperature fluctuation.

ACKNOWLEDGMENTS

We thank K. Sigurdson for useful discussions. This work was supported in part by NSF AST-0096023, NASA NAG5-8506, and DoE DE-FG03-92-ER40701.

-
- [1] L. Knox, Phys. Rev. D **52**, 4307 (1995); G. Jungman, M. Kamionkowski, A. Kosowsky, and D. N. Spergel, Phys. Rev. D **54**, 1332 (1995); J. R. Bond, G. Efstathiou, and M. Tegmark, Mon. Not. Roy. Astron. Soc. **296**, L33 (1997); M. Zaldarriaga, D. N. Spergel, and U. Seljak, Astrophys. J. **488**, 1 (1997); D. J. Eisenstein, W. Hu, and M. Tegmark, Astrophys. J. **518**, 2 (1999).
- [2] P. J. E. Peebles and J. T. Yu, Astrophys. J. **162**, 815 (1970); R. A. Sunyaev and Ya. B. Zel'dovich, Astrophys. Space Sci. **7**, 3 (1970); J. Silk, Astrophys. J. **151**, 459 (1968); see recent review by W. Hu and S. Dodelson, Annu. Rev. Astron. and Astrophys. **40**, 171 (2002).
- [3] A. D. Miller et al., Astrophys. J. Lett. **524**, L1 (1999); P. de Bernardis et al., Nature **404**, 955 (2000); S. Hanany et al., Astrophys. J. Lett. **545**, L5 (2000); N. W. Halverson et al., Astrophys. J. **568**, 38 (2002).
- [4] See, for example, A. Cooray, "Cosmology and Elementary Particle Physics: Coral Gables Conference on Cosmology and Elementary Particle Physics," eds. B. Kursunoglu, S. Mintz, and A. Perlmutter, AIP Proceedings **624**, 141 [arXiv:astro-ph/0203048].
- [5] B. S. Mason et al., preprint [arXiv: astro-ph/0205384].
- [6] R. A. Sunyaev and Ya. B. Zel'dovich, Mon. Not. Roy. Astron. Soc. **190**, 413 (1980).
- [7] J. R. Bond et al., preprint [arXiv: astro-ph/0205386].
- [8] E. Komatsu and U. Seljak, preprint [arXiv: astro-ph/0205468].
- [9] A. Cooray and A. Melchiorri, preprint [arXiv: astro-ph/0204250].
- [10] K. Sigurdson, A. Cooray, and M. Kamionkowski, in preparation.
- [11] M. Zaldarriaga, Phys. Rev. D **55**, 1822 (1997).
- [12] M. Zaldarriaga and U. Seljak, Phys. Rev. D **58**, 023003 (1998).
- [13] M. Kamionkowski, A. Kosowsky, and A. Stebbins, Phys. Rev. D **55**, 7368 (1997); Phys. Rev. Lett. **78**, 2058 (1997); M. Zaldarriaga and U. Seljak, Phys. Rev. D **55**, 1830 (1997).
- [14] M. Kamionkowski and A. Loeb, Phys. Rev. D **56**, 4511 (1997).
- [15] W. Hu, Astrophys. J. **529**, 12 (2000).
- [16] A. Cooray and R. Sheth, Phys. Reports, in press, preprint [arXiv: astro-ph/0206508].
- [17] E. Komatsu and T. Kitayama, Astrophys. J. **526**, L1 (1999).
- [18] A. Cooray, Phys. Rev. D **62**, 103506 (2000).
- [19] S. Y. Sazonov and R. A. Sunyaev, Mon. Not. Roy. Astron. Soc. **310**, 765 (1999).
- [20] A. Challinor, M. Ford, and A. Lasenby, Mon. Not. Roy. Astron. Soc. **312**, 159 (2000). E. Audit, J. F. L. Simmons, Mon. Not. Roy. Astron. Soc. **305**, L27 (1999).
- [21] A. Kosowsky, Ann. Phys. **246**, 49 (1996).
- [22] D. Limber, Astrophys. J. **119**, 655 (1954).
- [23] S. Cole and N. Kaiser, Mon. Not. Roy. Astron. Soc. **233**, 637 (1988).
- [24] W. H. Press and P. Schechter, Astrophys. J. **187**, 425 (1974).
- [25] H. J. Mo, B. Jain, and S. D. M. White, Mon. Not. Roy. Astron. Soc. **276**, L25 (1995).
- [26] J. P. Henry, Astrophys. J. **534**, 565 (2000).
- [27] W. Hu and D. J. Eisenstein, Phys. Rev. D **59**, 083509 (1999).
- [28] E. F. Bunn and M. White, Astrophys. J. **480**, 6 (1997).
- [29] C. L. Bennett et al., Astrophys. J. **436**, 423 (1994).
- [30] A. Cooray, Phys. Rev. D **64**, 063514 (2001).
- [31] See, for example, M. Kamionkowski and A. Kosowsky, Annu. Rev. Nucl. Part. Sci. **49**, 77 (1999), and references therein.
- [32] M. Kesden, A. Cooray, and M. Kamionkowski, Phys. Rev. Lett. **89**, 011304 (2002).
- [33] L. Knox and Y. S. Song, Phys. Rev. Lett. **89**, 011303 (2002).
- [34] A. Cooray and M. Kesden, preprint [arXiv: astro-ph/0204068].
- [35] U. Seljak and M. Zaldarriaga, Phys. Rev. Lett. **82**, 2636 (1999); W. Hu, Phys. Rev. D **64**, 083005 (2001).